Bull. Mater. Sci., Vol. 38, No. 7, December 2015, pp. 1749–1755. © Indian Academy of Sciences.

Structural, morphological and magnetic properties of $La_{1-x}Na_yMnO_3$ ($y \leq x$) nanoparticles produced by the solution combustion method

C O EHI-EROMOSELE[1,*], B I ITA[1,2], K O AJANAKU[1], A EDOBOR-OSOH[1], O ALADESUYI[1], S A ADALIKWU[2] and F E EHI-EROMOSELE[3]

[1]Department of Chemistry, Covenant University, PMB 1023, Ota 112264, Nigeria
[2]Department of Pure and Applied Chemistry, University of Calabar, Calabar 540213, Nigeria
[3]Department of Mechanical Engineering, University of Benin, Benin City 300271, Nigeria

MS received 15 June 2015; accepted 30 July 2015

Abstract. **The rapid solution combustion synthesis and characterization of sodium (Na)-substituted $LaMnO_3$ phases at relatively low temperature using polyvinyl alcohol (PVA) as fuel were reported. The thermal decomposition process investigated by means of differential and thermal gravimetric analysis (TG–DTA) showed that the use of PVA as a fuel was satisfactory in the synthesis of the perovskite manganite compound. Structural study using X-ray diffraction showed that all the samples were single phasic without any detectable impurities within the measurement range. Also, the Na-substituted compounds crystallize with rhombohedral symmetry (space group R-3c, no. 167) with $La_{0.80}Na_{0.15}MnO_3$ manganite sample giving the highest crystallinity. Microstructural features observed by field-emission scanning electron microscopy demonstrated that most of the grains were nearly spherical in shape with fairly uniform distribution and all the observed particles connect with each other. Energy-dispersive X-ray analyses confirm the homogeneity of the samples. Increase in magnetic moment was observed with the increase in sodium doping. Room-temperature vibrating sample magnetometer measurements showed that the samples were ferromagnetic with compositions $y = 0.10$, 0.15 and 0.20 showing relatively high magnetic moments of 33, 34 and 36 emu g^{-1}, respectively.**

Keywords. **Na-doped lanthanum manganites; solution combustion method; nanoparticles; magnetism.**

1. Introduction

There has been a surge in the studies of doped mixed valent perovskite manganese oxides in the past two decades owing to their colossal-magnetoresistance (CMR) effect near the Curie temperature T_c, charge and spin order as well as their potential applications.[1–10] Manganite perovskites have the general formula $R_{1-x}A_xMnO_3$ (where R is a rare earth cation and A the doping cation). Undoped $LaMnO_3$ manganite is an insulator having A-type antiferromagnetic ordering. By substitution of La^{3+} with a divalent or monovalent cation, $LaMnO_3$ can be driven into a metallic and ferromagnetic (FM) state.[11] These unusual and interesting changes observed in the properties of mixed valent manganites have been traditionally explained by the Zener double exchange (ZDE) mechanism[12] and in recent times various other factors such as the strong electron–phonon interaction,[10,13] the charge and orbital ordering,[14] the average sizes of the R and A cations[15,16] and the oxygen stoichiometry[10,17,18] have also been implicated.

Even though most studies on manganite perovskites have been centred on systems (A = Ca, Sr and Ba) in which a rare earth cation is substituted by A (divalent cation); studies on the substitution by monovalent cation (A = K, Ag, Na and Li) are presently attracting great interest.[10,11,19,20] It is well known that the ratio of Mn^{3+}/Mn^{4+} is an important factor in insulator to metal (I–M) and magnetic phase transitions in manganites. Monovalent cation doping is known to have a doubling effect on Mn valence state because of the charge difference as compared to divalent cation doping and hence the cation valency distribution can be represented as $La^{3+}_{1-x}Na^{+}_{x}$ $(Mn^{3+}_{1-2x}Mn^{4+}_{2x})O_3$.[10] The result is a small amount of Na doping that causes a large number of charge carriers and a consequent increase in the conductivity which also imparts on other physical properties. In particular, Na-doped lanthanum manganites (LNMO) have been shown to have large T_c as well as large magnetoresistance values near room temperature which renders these compounds as promising functional materials for information technologies, medicine and low-temperature thermal engineering.[8,21]

The dependence of the physical and chemical properties of nanocrystalline materials on the shape and size of nanoparticles and the thermal history of sample preparation as well have always motivated the study of new synthetic routes to produce these materials. This is a key factor since the effective morphology, the chemical composition and the grain size distribution deeply affect the physico-chemical properties of the materials prepared by the various currently preparative routes for obtaining materials with grains of the

*Author for correspondence (cyril.ehi-eromosele@covenantuniversity.edu.ng)

order of few tens of nanometres.[21] Hence the synthesis, sintering, and characterization of the nanostructured materials have become a vital part of ceramic research. Particularly, the synthesis of oxides with perovskite crystal structure requires high temperature (≥ 700°C). This creates difficulties in terms of shape and individual properties of particles[22] as a result, soft chemical methods of synthesis will offer some advantages in this regard. The solution combustion method offers an advantage over other conventional methods in that it is a low-temperature initiated exothermic and self-propagating process. Combustion reaction is a vigorous exothermic redox reaction between a suitable fuel which also acts as a complexing agent and an oxidizer (i.e., corresponding metal nitrates). Combustion synthesis has the advantage of high temperatures, fast heating rates and short reaction times thus inhibiting particle size growth and promoting the formation of homogeneous, crystalline nanopowders.

Numerous papers[1,8,10,11,23] have been devoted to the structure and properties of Na-doped lanthanum manganites which have been mainly produced by the solid-state synthetic route. It is important to note that the loss of Na can occur during the long sintering process associated with solid-state synthesis.[24] There is a paucity of reports in literature on Na-doped lanthanum manganites synthesized through the combustion route. Nanocrystalline Na-doped lanthanum manganites have been produced by the combustion method using urea[21] and oxalyl dihydrazide[25] as fuels. In the present study, a series of ferromagnetic Na-doped lanthanum manganites by the solution combustion method has been synthesized at relatively low temperatures using polyvinyl alcohol (PVA) as a fuel. X-ray diffraction (XRD), differential and thermal gravimetric analysis (TG-DTA), field emission scanning electron microscopy (FE-SEM), energy-dispersive X-ray (EDAX) analyses and vibrating sample magnetometer (VSM) techniques are used to study the structural, morphological, chemical composition and magnetic properties of $La_{1-x}Na_yMnO_3$ ($y \leq x$) ceramic manganite sample, respectively.

2. Experimental

2.1 *Combustion synthesis*

Polycrystalline samples of $La_{1-x}Na_yMnO_3$ ($y \leq x$) with nominal y-values of 0.1, 0.15 and 0.2 have been prepared by the solution combustion synthetic route using PVA as fuel. In the synthesis of the different compositions of $La_{1-x}Na_yMnO_3$, fuel stoichiometric composition was used. For $y = 0.1$ sample, 3.46 g $La(NO_3)_3{\cdot}6H_2O$ (99.9% purity from Alfar Aesar, USA), 0.09 g $NaNO_3$ (99.9+% purity from Aldrich), 2.51 g $Mn(NO_3)_2{\cdot}4H_2O$ (99.9+% purity from Aldrich) and 0.99 g PVA (MW: ~125,000 from SD Fine Chem. Ltd., Mumbai) were dissolved in 20 ml of distilled water and the solutions were heated to 80°C to form a viscuous gel of precursors under magnetic stirring. After that, the gel was transferred to a pre-heated coil (300°C). Finally, after a short moment, the solution precursors boiled, swelled, evolved a large amount of gases and ignited, followed by the yielding of puffy black products. The autocombusted powder was annealed at 800°C for 5 h in air and used for further characterization. Similarly, for $y = 0.15$ sample, same procedures were followed except that 0.13 g $NaNO_3$ and 1.00 g PVA were used as precursors whereas for $y = 0.2$ sample, 0.17 g $NaNO_3$ and 1.01 g PVA were used.

2.2 *Characterization methods*

The precursor gel was characterized by TG–DTA by means of STA 409 PC Luxx simultaneous DSC–TG–DTA instrument from NETZSCH-Geratebau Germany at a temperature range of 30–1000°C in air atmosphere with a heating rate of 10°C min^{-1}. The X-ray diffractograms of the annealed powders were recorded using an X-ray diffractometer (D8 Advance, Bruker Germany), equipped with a Cu Kα radiation source ($\lambda = 1.5406$ Å) and the crystallite size (D) is calculated from X-ray line broadening of the (110) diffraction peak using the well-known Scherrer relation

$$D = \frac{0.9\lambda}{\beta \cos\theta}, \tag{1}$$

where β is the full-width at half-maxima of the strongest intensity diffraction peak (311), λ the wavelength of the radiation, and θ the angle of the strongest characteristic peak. The surface morphology and chemical composition were examined with a FE-SEM using FEI NOVA NANO SEM 600. The magnetic characterizations were carried out with a vibrating scanning magnetometer (Lake Shore cryotronics-7400 series) under the applied field of $\pm 20{,}000G$ at room temperature.

3. Results and discussion

3.1 *Combustion reaction*

Assuming complete combustion, the theoretical general equation for the formation of $La_{1-x}Na_yMnO_3$ ($y \leq x$) nanoparticles can be written as follows:

$$\begin{aligned}&(1-x)\,La\,(NO_3)_{3(aq)} + yNaNO_{3(aq)} + Mn\,(NO_3)_{2(aq)} \\ &+ (\sim C_2H_4O)_{n(aq)} + (9.99-10)\,O_2 \\ &\rightarrow \mathbf{La_{1-x}Na_yMnO_{3(aq)}} + CO_{2(g)}\uparrow + H_2O_{(g)}\uparrow \\ &+ N_{2(g)}\uparrow.\end{aligned} \tag{2}$$

The precursor solutions were foamy and white coloured which turned sooty black after combustion. In all samples, the combustion types were flamy combustion. After annealing at 800°C for 5 h, the powders became finer and were used for further characterizations.

3.2 *Thermal analysis*

The autocatalytic nature of the combustion process in which the nitrate ions act as an oxidizer while the PVA fuel plays

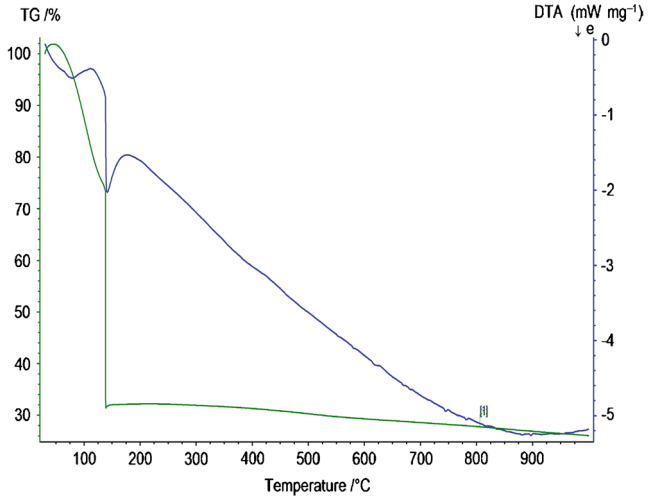

Figure 1. TG–DTA curves for the precursor gel of $La_{0.8}Na_{0.2}MnO_3$ sample.

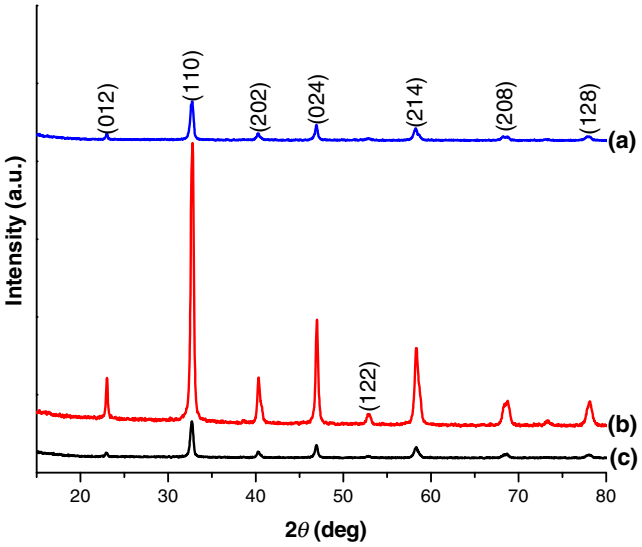

Figure 2. XRD patterns of (**a**) $La_{0.8}Na_{0.1}MnO_3$, (**b**) $La_{0.8}Na_{0.15}MnO_3$ and (**c**) $La_{0.8}Na_{0.2}MnO_3$ samples.

the role of a reducer was investigated by TG–DTA measurements. The simultaneous TG–DTA curves for the stoichiometric precursor gel (for $La_{0.8}Na_{0.2}MnO_3$ sample) were recorded in a temperature range of 35–1000°C and it is shown in figure 1. The TG curve shows a weight loss of about 26% below 130°C which is due to complete evaporation of water in the precursor gel. The sudden weight loss of 42% was observed at about 130°C and it is attributed to the rapid chemical reaction between the metal nitrates and PVA. This maximum weight loss occurs at a definite temperature (130°C) indicating the occurrence of combustion reaction during the decomposition step of the nitrate–PVA dried gel. The requirement of lower temperature for the combustion reaction using PVA as a fuel may be due to the release of maximum energy from the stoichiometric composition of redox mixture of the metal nitrates and PVA leading to the decomposition of the gels below the melting point of PVA (200°C). No significant weight loss is observed after the combustion reaction indicating the formation of a perovskite phase with a yield of about 32%. The thermogravimetric (TG) study of precursors reveals that the stable phase formation takes place at temperatures above 600°C. However, the formation of a perovskite phase still has to be confirmed by XRD analysis. The result shows that the use of PVA as a fuel is satisfactory in the synthesis of the perovskite manganite compound. The DTA curves complement the weight loss regime reported in the TG. The endothermic peak at about 100°C was attributed to the complete evaporation of water and organic content in the precursor gel while the sharp exothermic peak observed in the DTA curve around 130°C was attributed to the ignition of nitrate–PVA precursors dried gel at this temperature.

3.3 *Structural and phase analysis*

Figure 2a–c shows the XRD patterns of the $La_{1-x}Na_yMnO_3$ samples. The analysis of the X-ray powder diffraction pattern shows the formation of homogeneous single-phase perovskite compounds. The obtained peaks are well matched to the rhombohedral perovskite structure having the lattice parameters $a = 5.4905$ Å, and $c = 13.3077$ Å with R-3c (167) space group. The average crystallite size obtained for samples $y = 0.1$, 0.15, and 0.2 are 44, 47 and 45 nm, respectively. The crystallite sizes of the samples obtained from this combustion method using PVA were comparable with the oxalyl dihydrazide-assisted combustion[25] but were smaller than the ones reported in literature for same sample using the solid-state synthetic route. XRD patterns of all the samples show that the reflection peaks are quite broad, indicating their nanocrystallinity. All samples show pure XRD peak (after annealing at 800°C for 5 h) with no secondary peak confirming the TG results. The splitting of the peaks (mostly the main 110 lines) of all samples was not as pronounced like their $La_{1-x}Na_xMnO_3$ analogues synthesized by solid-state route.[10,11] The XRD analysis of $La_{1-x}Na_xMnO_3$ samples shows that the splitting of the main (110) lines decreases and seems to merge into one line with oxygen stoichiometry.[10] It is very likely that these $La_{1-x}Na_yMnO_3$ samples are/or near oxygen stoichiometric. However, the chemical composition still has to be confirmed by EDAX analysis. There is a variation of the crystallinity of the perovskite phase with the $La_{0.8}Na_{0.15}MnO_3$ sample recording the highest (indicated by the intensity of its peaks). Sodium appears in the perovskite structure, substituting vacancies in the A sub-lattice (i.e., in the lanthanum sub-lattice). Thus, compositions like $y = 0.2$ ($La_{0.8}Na_{0.2}MnO_3$) are compounds with a completely filled A sub-lattice, in which lanthanum and sodium ions are statistically distributed over A positions. Intermediate compositions like $y = 0.1$ ($La_{0.8}Na_{0.1}MnO_3$) and $y = 0.15$ ($La_{0.8}Na_{0.15}MnO_3$) are compounds with partly filled A sub-lattice, in which the remaining positions are vacancies. Such sodium-deficient compounds can be obtained with

improved transport characteristics since they permit high fritting temperatures without precipitation of sodium in view of their high thermodynamic stability as compared to compounds with higher sodium content.[26] Better physical properties were also recorded for $La_{0.8}Ag_{0.15}MnO_3$ manganite despite the non-stoichiometry of the composition compared to $La_{0.85}Ag_{0.15}MnO_3$ manganite.[27] In all probabilities, it is possible that the $y = 0.15$ sample satisfied this requirement hence its higher crystallinity (indicating higher perovskite phase) than the other samples.

3.4 *Morphological and chemical composition analysis*

The surface morphologies of the samples were analysed by FE-SEM and the images for samples $y = 0.1$, 0.15 and 0.2 are shown in figure 3a–c, respectively. The samples show that most of the grains are nearly spherical in shape with fairly uniform distribution and all the observed particles connect with each other. Similar morphology was observed in the $La_{1-x}Na_xMnO_3$ samples synthesized using conventional solid-state reaction route.[11] The appearance of voids in the microstructure of the samples might be due to escaping large number of gases during the combustion reaction characteristic of nanoparticles synthesized by the combustion method. The formation of multigrain agglomerates observed in all the samples consists of very fine crystallites as they show strong tendency to form agglomerates.

The compositional analysis of the nanocrystalline $La_{1-x}Na_yMnO_3$ ($y = 0.1$, 0.15 and 0.2) samples were carried out by EDAX. Representative EDAX spectra for $y = 0.15$ is shown in figure 4. From the EDAX results, the presences of La, Na, Mn and O in the samples were confirmed. The spectra indicate that all the samples (table 1) are consistent with their elemental signals and stoichiometry close to the nominal composition (table 2) thereby having a broad homogeneity area. The spectra analysis also revealed nearly ideal oxygen stoichiometry even though actual oxygen content of the samples have to be checked by iodometric titrations which was not considered in this study.

3.5 *Magnetic studies*

The specific magnetization curves of the $La_{1-x}Na_yMnO_3$ samples obtained from room-temperature VSM measurements are shown in figure 5a–c. The magnetic properties of the $La_{1-x}Na_yMnO_3$ powders are given in table 2. Figure 5a–c shows curves that are typical of a soft magnetic material and indicate hysteresis loops. From these measurements, saturation magnetization (M_s), remanence (M_r), coercivity (H_c) and squareness ratio (M_r/M_s) were derived

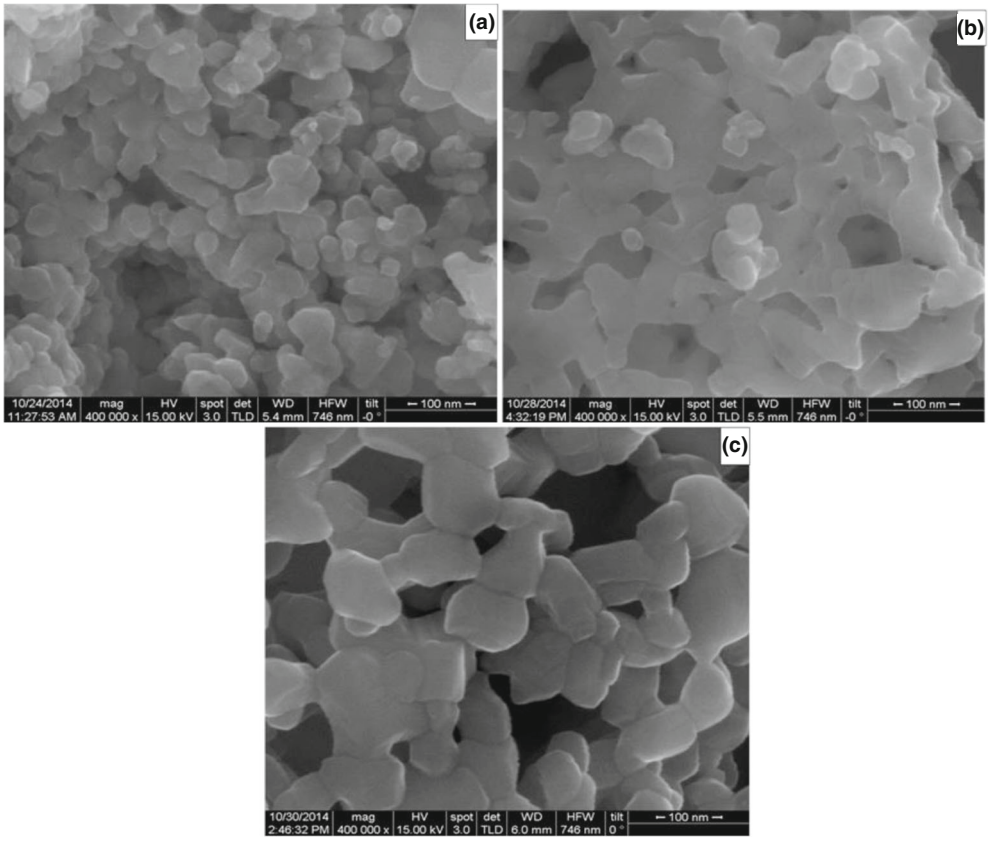

Figure 3. FE-SEM images of (**a**) $La_{0.8}Na_{0.1}MnO_3$, (**b**) $La_{0.8}Na_{0.15}MnO_3$ and (**c**) $La_{0.8}Na_{0.2}MnO_3$ samples.

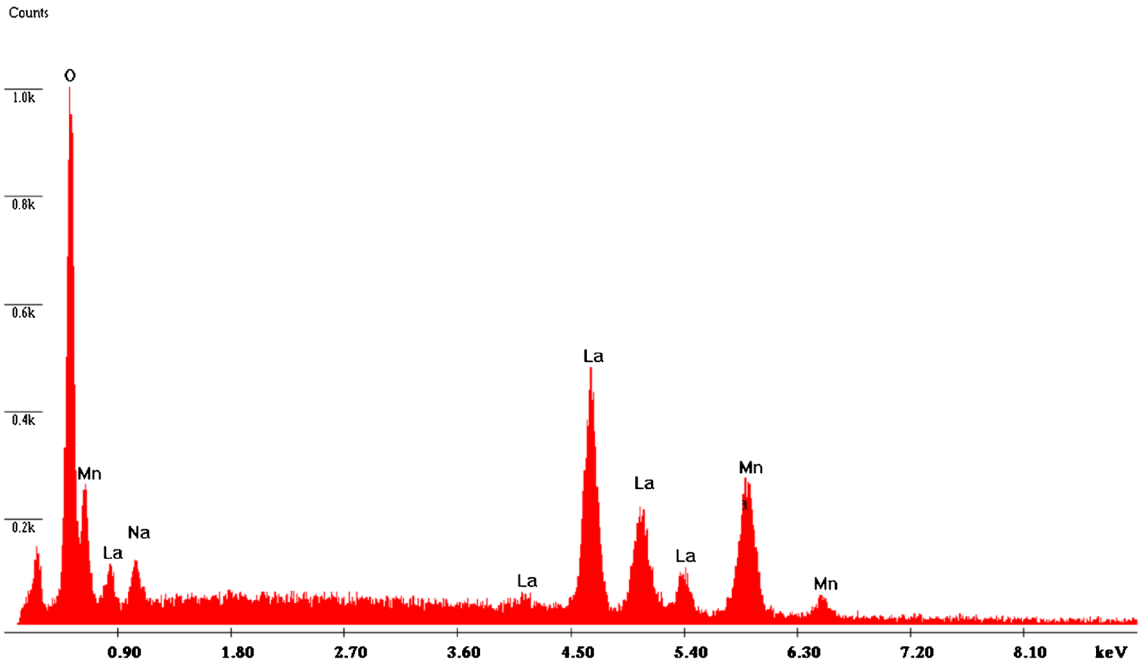

Figure 4. EDAX spectra of $La_{0.8}Na_{0.15}MnO_3$ sample.

Table 1. Per cent concentration of the constituent elements of $La_{1-x}Na_yMnO_3$ ($y \leq x$) system by EDAX.

Sample	La	Na	Mn	O
$y = 0.1$	16.22	2.01	20.34	61.43
$y = 0.15$	16.12	3.00	20.10	60.78
$y = 0.2$	15.85	4.01	19.96	60.18

Table 2. Magnetic properties of $La_{1-x}Na_yMnO_3$ ($y \leq x$) powders.

Sample	Saturation magnetization, M_s (emu g^{-1})	Remanence magnetization, M_r (emu g^{-1})	Coercivity, H_c (G)	M_r/M_s
$y = 0.1$	33	15.50	167	0.470
$y = 0.15$	34	16	146	0.471
$y = 0.2$	36	17	138	0.472

and listed in table 2. The ferromagnetism seen in LNMO comes from the doping of the parent perovskite manganite ($LaMnO_3$) by the replacement of La with Na. Compounds of the $La_{1-x}Na_yMnO_3$ ($y \leq x$) type differ from other systems, in which divalent metal ions play the role of doping elements, in that they contain in addition to y two-charged acceptors (Na^+ ions), also $x-y$ three charged acceptors (La^{3+} vacancies), which also form a high conductivity ferromagnetic state, inducing the $Mn^{3+} \rightarrow Mn^{4+}$ transition.[26] Saturation magnetization (M_s) is the state where an increase in magnetizing force produces no further increase in magnetic induction in a magnetic material. The magnetization remains in the sample even after the applied field reduced to zero is termed as a remanent magnetization (M_r). Both

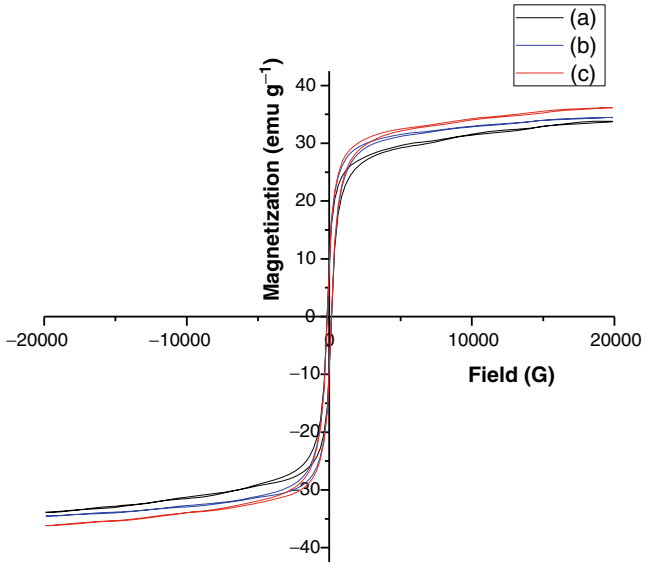

Figure 5. Magnetic hysteresis curves measured at room temperature of (**a**) $La_{0.8}Na_{0.1}MnO_3$, (**b**) $La_{0.8}Na_{0.15}MnO_3$ and (**c**) $La_{0.8}Na_{0.2}MnO_3$ samples.

M_r and M_s are the important parameters to be considered in the study of magnetic behaviour of magnetic materials. Remanence is a structure-sensitive parameter.[28] It can be seen that all the samples possess ferromagnetic behaviour at room temperature. Also, the results show that M_s and M_r increased with the increase in Na^+ doping. Similar results were observed with $La_{1-x}Na_xMnO_3$ samples with $x \leq 0.2$[25] and $x \leq 0.15$[11] and in $La_{1-x}Ag_xMnO_3$ samples with $x \leq 0.2$.[29] It is known that the substitution of Na^+ (y) produces ($2y$) Mn^{4+} leading to enhanced hole density, strengthening

of the ZDE mechanism and hence increased ferromagnetism (as shown by increased M_s values). The ratio of Mn^{3+}/Mn^{4+} is an important factor to show I–M transition and magnetic phase transition in manganites. It is important to state that increased Na^+ doping level ($y \geq 0.2$) leads to a reduction in ferromagnetism.[8,25] From the crystallite sizes of the samples, one would expect the $La_{0.8}Na_{0.15}MnO_3$ ($y = 0.15$) sample, with the highest crystallite size (47 nm) of all samples, to present the highest magnetic moment (table 2). The effect of grain size on the magnetic properties of manganites has been widely reported.[25,30–32] These studies suggest that magnetic moment increases with the increase in the particle size of manganites. But in this study, the ZDE mechanism clearly accounts for the increase in magnetic moment observed with increased Na^+ doping. The results also show that the H_c was affected by Na^+ doping. H_c increased with the increase in Na^+ doping. The saturation magnetization is related to H_c through Brown's relation,[33] $H_c = 2K1/\mu_o M_s$. According to this relation, H_c is inversely proportional to M_s, which is consistent with our experimental results. M_r/M_s values are found to be around 0.5 for all samples which is the expected value for randomly packed single domain particles.[28]

4. Conclusion

In conclusion, low-temperature auto-combustion synthesis of Na-substituted lanthanum manganite perovskite nanoparticles is reported. A series of $La_{1-x}Na_yMnO_3$ ($y \leq x$) were successfully prepared with different concentrations of Na ($y = 0.1$, 0.15 and 0.2) for a detailed structural and magnetic study. The TG study of precursors reveals that the stable phase formation takes place at temperatures above 600°C and that the use of PVA as a fuel is satisfactory in the synthesis of the perovskite manganite compound. XRD confirmed the formation of nanocrystalline perovskite pure-phase with no impurity phase in all the samples studied. The obtained peaks are well matched to the rhombohedral perovskite structure. Despite the nonstoichiometry of the composition, the $La_{0.80}Na_{0.15}MnO_3$ manganite sample gave the highest crystallinity highlighting their high thermodynamic stability. The samples show that most of the grains are nearly spherical in shape with fairly uniform distribution and all the observed particles connect with each other. The EDAX spectra indicate that all the samples are consistent with their elemental signals and stoichiometry close to the nominal composition thereby having a broad homogeneity area. All samples recorded a fairly high saturation magnetization (33–36 emu g^{-1}) with M_s, M_r and H_c increasing with increased Na^+ doping. This increase in magnetic moment of the samples with increased Na^+ doping has been discussed in the context of enhanced hole density and strengthening of the ZDE mechanism.

Acknowledgements

This work would not have been possible without the visiting research grant given to Mr Ehi-Eromosele CO by the International Centre for Materials Science, Jawarharlal Nehru Centre for Advanced Scientific Research, Bangalore, India. The corresponding author would like to thank Professor Vikram Jayaram, Chairman of the Department of Materials Engineering, Indian Institute of Science (IISc), Bangalore, for giving access to the VSM and TG-DTA facilities in his department, as well thank Mr Olu Emmanuel Femi for introducing him to Professor Vikram Jayaram.

References

1. Varshney D, Dodiya N and Shaikh M W 2011 *J. Alloys Compd.* **509** 7447
2. Mansuri I and Varshney D 2012 *J. Alloys Compd.* **513** 256
3. Cheikh-Rouhou Koubaa W, Koubaa M and Cheikhrouhou A 2009 *J. Alloys Compd.* **470** 42
4. Wang H, Zhang X, Hundley M F, Thompson J D, Gibbons B J, Lin Y, Arendt P N, Foltyn S R and Jia Q X 2004 *Appl. Phys. Lett.* **84** 1147
5. Tan G, Zhang X and Chen Z 2004 *J. Appl. Phys.* **95** 6322
6. So J H, Gladden J R, Hu Y F, Maynard J D and Li Q 2003 *Phys. Rev. Lett.* **90** 036103-1
7. Coey J M D, Viret M and Molnar S V 1999 *Adv. Phys.* **48** 167
8. Roy S, Guo Y Q, Venkatesh S and Ali N 2001 *J. Phys.: Condens. Matter* **13** 9547
9. Urushibara A, Moritomo Y, Arima T, Asamisu A, Kido G and Tokura Y 1995 *Phys. Rev. B* **51** 14103
10. Malavasi L, Mozzati M C, Ghigna P, Azzoni C B and Flor G 2003 *J. Phys. Chem. B* **107** 2500
11. Kansara S B, Dhruv D, Kataria B, Thakera C M, Rayaprol S, Prajapat C L, Singh M R, Solanki P S, Kuberkar D G and Shah N A 2015 *Ceram. Int.* **41** 7162
12. Zener C 1951 *Phys. Rev.* **81** 440
13. Millis A J, Littlewood P B and Shraiman B I 1995 *Phys. Rev. Lett.* **74** 5144
14. Chen C H and Cheong S-W 1996 *Phys. Rev. Lett.* **78** 4253
15. Hwang H Y, Cheong S-W, Radaelli P G, Marezio M and Battlogg B 1995 *Phys. Rev. Lett.* **75** 914
16. Sun J R, Rao G H, Gao X R, Liang J K, Wong H K and Shen B G 1999 *J. Appl. Phys.* **85** 3619
17. Mitchell J F, Argyriou D N, Potter C D, Hinks D G, Jorgensen J D and Bader S D 1996 *Phys. Rev. B* **54** 6172
18. Li T, Wang B, Dai H, Du Y, Yan H and Liu Y 2005 *J. Appl. Phys.* **98** 123505
19. Gorbenko O Yu, Markelova M N, Melnikov O V, Kaul A R, Atsarkin V A, Demidov V V, Mefed A E, Roy E J and Odintsov B M 2009 *Dokl. Chem.* **424** 7
20. Sukhorukov Yu P, Telegin A V, Bessonov V D, Gan'shina E A, Kaul A R, Korsakov I E, Perov N S, Fetisov L Yu and Yurasov A N 2014 *J. Magn. Magn. Mater.* **367** 53
21. Malavasi L, Mozzati M C, Polizzi S, Azzoni C B and Flor G 2003 *Chem. Mater.* **15** 5036

22. Melnikov O V, Gorbenko O Y, Markelova M N, Kaul A R, Atsarkin V A, Demidov V V, Soto C, Roy E J and Odintsov B M 2009 *J. Biomed. Mater. Res. A* **91** 1048
23. Ghigna P, Carollo A, Flor G, Malavasi L and Peruga G S 2005 *J. Phys. Chem. B* **109** 4365
24. Rao G H, Sun J R, Barner K and Hamad N 1999 *J. Phys.: Condens. Matter* **11** 1523
25. Shivakumara C, Bellakki M B, Prakash A S and Vasanthacharya N Y 2007 *J. Am. Ceram. Soc.* **90** 3852
26. Kamilov I K, Gamzatov A G, Aliev A M, Batdalov A B, Abdulvagidov Sh B, Melnikov O V, Gorbenko O Yu and Kaul A R 2007 *J. Exp. Theor. Phys.* **105** 774
27. Abdulvagidov Sh B, Gamzatov A G, Melnikov O V and Gorbenko O Yu 2009 *J. Exp. Theor. Phys.* **109** 989
28. Salunkhe A B, Khot V M, Phadatare M R, Thorat N D, Joshi R S, Yadav H M and Pawar S H 2014 *J. Magn. Magn. Mater.* **352** 91
29. Bellakki M B, Shivakumara C, Vasanthacharya N Y and Prakash A S 2010 *Mater. Res. Bull.* **45** 1685
30. Wang J, Gu B, Sang H, Ni G and Du Y 2001 *J. Magn. Magn. Mater.* **223** 50
31. Yang J, Zhao B C, Zhang R L, Ma Y Q, Sheng Z G, Song W H and Sun Y P 2004 *Solid State Commun.* **132** 83
32. Hueso L E, Rivadulla F, Sanchez R D, Caeiro D, Jardon C, Vazquez-Vazquez C, Rivas J and Lopez-Quintela M A 1998 *J. Magn. Magn. Mater.* **189** 321
33. Coey J M D 1996 *Rare earth permanent magnetism* (New York: Wiley)